

# Articles

## Synthesis of Silicon-Bridged Benzocrown Ethers and Their Ionochromism in the Emission Spectra Arising from Intramolecular $\pi$ – $\pi$ Stacking

Joji Ohshita,\* Taisuke Uemura, Takahiro Inoue, Toshiyuki Iida, and Atsutaka Kunai\*

Department of Applied Chemistry, Graduate School of Engineering, Hiroshima University, Higashi-Hiroshima 739-8527, Japan

Received June 23, 2004

Compounds having two benzocrown ether units bridged by a mono-, di-, or trisilanylene unit were prepared, and ionochromic effects on their optical properties were studied. Of these, disilanylene- and trisilanylene-bridged ones exhibited clear ionochromism in the emission spectra and the intensity of the original emission band at about 320 nm decreased and a new broad band centered at 400 nm appeared when appropriate alkali or alkali-earth metal ions were added into the acetonitrile solutions. In contrast, a monosilanylene-bridged benzocrown ether and a disilanylbenzocrown ether showed ionochromic changes in different fashions, indicating that the new emission band at low energy of the di- and trisilanylene-bridged benzocrown ethers in the presence of metal ions may be ascribed to the intramolecular  $\pi$ – $\pi$  stacking. MO calculations were carried out to understand the ionochromism.

### Introduction

Compounds and polymers having  $\pi$ -conjugated carbon units linked by an organosilanylene  $\sigma$ -bond linkage are of interest because they are usable as functionality materials, such as carrier transports and photoluminescent materials.<sup>1,2</sup> In these molecules, orbital interaction between the silicon  $\sigma$ - and carbon  $\pi$ -orbitals ( $\sigma$ – $\pi$  conjugation) takes place, leading to red-shifted UV absorption and emission maxima from those of the parent  $\pi$ -conjugated molecules.

Several approaches have been examined to develop  $\pi$ -conjugated molecules that respond to metal ions, for use as ion sensors.<sup>3,4</sup> Silicon-based ion-sensing molecules also have been studied, recently. West and co-workers found that a polysilane featuring ether side chains responds to  $\text{Li}^+$  with respect to absorption and emission

spectra, arising from conformational changes.<sup>5</sup> Kira et al. demonstrated that *p*-disilanylacetophenone shows dual emission depending on the presence of  $\text{Lu}^{3+}$  and  $\text{Sc}^{3+}$ , due to intramolecular charge transfer induced by the complex formation with the metal ions.<sup>6</sup> In the hope of developing ion-sensing materials based on the Si– $\pi$  system, we recently synthesized thienylene–disilanylene alternating oligomers having linear ether side chains on the thiophene rings.<sup>7</sup> In these studies, coordination of the polymer side chains with metal ions was anticipated to cause significant conformational changes in the flexible thienylene–disilanylene units, which would affect the nature of the  $\sigma$ – $\pi$  conjugation, leading to chromic behaviors. In addition, silicon substitution enhances the emission efficiencies of the fluorophores in some cases, which may allow the use of silicon-substituted  $\pi$ -conjugated compounds and polymers as photoluminescent materials.<sup>2a,8</sup> Although the thienylene–disilanylene oligomers exhibited unique solvatochromic behaviors in the emission spectra in the solution phase, they did not respond to coexisting metal ions, despite our expectation. This was presumably due to the weak coordination of linear ether chains with metal ions. In this paper, we report the synthesis of compounds having two benzocrown ether units bridged by an organosilicon

(1) For review, see: (a) Ohshita, J.; Kunai, A. *Acta Polym.* **1998**, *49*, 379. (b) Uhlig, W. *Prog. Polym. Sci.* **2002**, *27*, 255.

(2) For recent works, see: (a) Mori, A.; Takahisa, E.; Yamamura, Y.; Kato, T.; Mudalige, A. P.; Kajiro, H.; Hirabayashi, K.; Nishihara, Y.; Hiyama, T. *Organometallics* **2004**, *23*, 1755. (b) Wang, F.; Kaafarani, B. R.; Neckers, D. C. *Macromolecules* **2003**, *36*, 8225. (c) Morisaki, Y.; Fujimura, F.; Chujo, Y. *Organometallics* **2003**, *22*, 3553. (d) Kwak, G.; Sumiya, K.; Sanda, F.; Masuda, Y. *J. Polym. Sci., A, Polym. Chem.* **2003**, *41*, 3615.

(3) For review, see: (a) Prodi, L.; Bolletta, F.; Montalti, M.; Zacheroni, N. *Coord. Chem. Rev.* **2000**, *208*, 59. (b) Valeur, B. *Molecular Fluorescence*; Wiley-VCH: New York, 2002.

(4) For recent example, see: (a) Bronson, R. T.; Bradshaw, J. S.; Savage, P. B.; Fuangswasdi, S.; Lee, S. C.; Krakowiak, K. E.; Izatt, R. M. *J. Org. Chem.* **2001**, *66*, 4752. (b) Strauss, J.; Daub, J. *Org. Lett.* **2002**, *4*, 683. (c) Kim, J.; Swager, T. M. *Angew. Chem., Int. Ed.* **2000**, *39*, 3868. (d) Baskar, C.; Lai, Y.-H.; Valiyaveetil, S. *Macromolecules* **2001**, *34*, 6255. (e) Wituski, B.; Weber, M.; Bergsträsser, U.; Desvergne, J.-P.; Bassani, D. M.; Bouas-Laurent, H. *Org. Lett.* **2001**, *3*, 1467. (f) Pasini, D.; Righetti, P. P.; Rossi, V. *Org. Lett.* **2002**, *4*, 23.

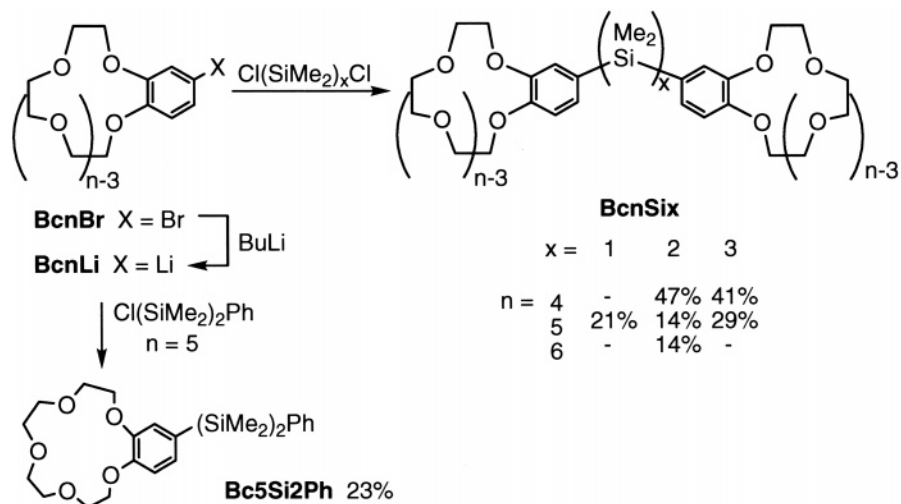
(5) Toyoda, S.; Fujiki, M.; Yuan, C.-H.; West, R. *Macromolecules* **2000**, *33*, 1503.

(6) Kira, M.; Badugu, R.; Li, T.-X.; Setaka, W.; Sakamoto, K.; Hashimoto, H. *Chem. Lett.* **2002**, 242.

(7) (a) Ohshita, J.; Hashimoto, M.; Kunai, A. *Organometallics* **2001**, *20*, 4296. (b) Ohshita, J.; Hashimoto, M.; Lee, K.-H.; Yoshida, H.; Kunai, A. *J. Organomet. Chem.* **2003**, *682*, 267.

(8) (a) Maeda, H.; Inoue, Y.; Ishida, H.; Mizuno, K. *Chem. Lett.* **2001**, 1224. (b) Kyushin, S.; Ikarugi, M.; Goto, M.; Hiratsuka, H.; Matsumoto, H. *Organometallics* **1996**, *15*, 1067.

Scheme 1. Synthesis of Benzocrown-Substituted Organosilanes



unit, in which the benzocrown ether units may coordinate strongly with metal ions.<sup>9,10</sup>

## Results

Silicon-bridged benzocrown ethers (**BcnSix**) were prepared by the reactions of the corresponding dichlorosilanes with lithiated benzocrown ethers (**BcnLi** in Scheme 1). The lithiated benzocrown ethers were thermally labile, and their THF solutions, upon standing, rapidly decomposed even at  $-90\text{ }^{\circ}\text{C}$ . Although chlorosilanes were added to the solutions of the lithiated benzocrown ethers immediately after the formation, yields of the silicon-bridged benzocrowns were rather low, ranging from 14% to 47%. 2-Phenyldisilanylbenzocrown ether (**Bc5Si2Ph**) was also prepared for comparison.

UV spectra of the present silicon-bridged benzocrown derivatives in acetonitrile (AN) revealed the maxima at lower energy (282–285 nm) than those of the respective benzocrown ethers (**BcnH**) ( $\lambda_{\text{max}} = 275\text{ nm}$  for **Bc4H**, 278 nm for **Bc5H**, and 277 nm for **Bc6H**). Addition of metal ions  $\text{Li}^+$ ,  $\text{Na}^+$ ,  $\text{Mg}^{2+}$ , and  $\text{Ca}^{2+}$  as the perchlorates in large excess led to slight blue shifts of the absorption maxima of **BcnSix** by 3–10 nm. However, the silicon chain length in these compounds did not affect the ionochromic behaviors, and similar blue shifts were observed when the metal ions were added into the solutions of **BcnH** and **Bc5Si2Ph**. Therefore, the blue shifts of the absorption maxima of **BcnSix** in response to metal ions seem to be characteristics of the benzocrown ether itself, but the silicon bridge did not play an important role in the ionochromic UV spectral changes of **BcnSix**.

In contrast to the UV absorption spectra, emission spectral profiles of di- and trisilanylene-bridged benzocrown derivatives in AN were markedly affected by

the coexistence of appropriate metal ions. Figure 1 represents the emission spectra of **BcnSix** ( $x = 2$  or 3) in the presence of a large excess of alkali and alkali-earth metal ions. As can be seen in Figure 1a, addition of the metal ions to solutions of **Bc4Si2** in AN resulted in a decrease of the intensity of the original emission band at 318 nm. Most evidently, when  $\text{Ca}^{2+}$  was added, the original band almost disappeared and a new broad band appeared around 410 nm, instead. This is in marked contrast to **Bc4H**, whose emission band moved to higher energies and was slightly enhanced by adding  $\text{Ca}^{2+}$ . The sensitivity of **Bc4Si2** concerning the emission spectral changes decreased depending on the metal ions, in the order  $\text{Ca}^{2+} > \text{Li}^+, \text{Na}^+ \gg \text{Mg}^{2+}$  (Figure 1a,f). Thus, **Bc4Si2** responded to  $\text{Li}^+$  and  $\text{Na}^+$ , less sensitively than to  $\text{Ca}^{2+}$ , to decrease the intensity to approximately one-fifth of that in the absence of the metal ions. No significant changes were observed when  $\text{Mg}^{2+}$  was added to a solution of **Bc4Si2**.

Addition of the ions to solutions of **Bc5Si2** also caused ionochromic changes in the emission spectra, and the degree of the changes decreased in the order  $\text{Ca}^{2+}, \text{Mg}^{2+} \gg \text{Li}^+, \text{Na}^+$ , as shown in Figure 1b,f. **Bc6Si2** exhibited clear ionochromism with  $\text{Ca}^{2+}$ , similar to **Bc4Si2** and **Bc5Si2**, but was much less sensitive to  $\text{Li}^+$ ,  $\text{Na}^+$ , and  $\text{Mg}^{2+}$  (Figure 1c,f). These results indicated that the ion-dependence of the chromic behaviors was markedly affected by the crown ether ring size. The silanylene chain length, i.e.,  $x = 2$  or 3, however, did not exert an influence on the order of ionochromic sensitivities depending on the ions, except that **Bc5Si3** responded to  $\text{Mg}^{2+}$  more sensitively than  $\text{Ca}^{2+}$ , in contrast to **Bc5Si2** (Figure 1b,e). **BcnSi3** always exhibited an enhanced emission band in the low-energy region in the presence of appropriate metal ions (Figure 1d,e), as compared with **BcnSi2**.

Figure 2a,b shows emission spectral changes on titration of **Bc4Si3** and **Bc5Si3** with  $\text{Ca}^{2+}$  and  $\text{Mg}^{2+}$  in AN, respectively, indicating that the continuous changes occurred through an isosbestic point with increasing the concentration of the metal ions, making it possible to utilize the present silicon-bridged benzocrown derivatives as novel ion-sensing reagents. For example, titration of **Bc4Si3** and **Bc5Si3** ( $x = 2$  or 3) with  $\text{Ca}^{2+}$  and

(9) For a preliminary communication, describing the synthesis and ionochromism of **Bc4Si2**, **Bc5Si1**, **Bc5Si2**, and **BcSi2Ph**, see: Ohshita, J.; Inoue, T.; Uemura, T.; Iida, T.; Kunai, A. *Silicon Chem.* **2002**, *1*, 383.

(10) For recent example of ion-sensing compounds bearing benzocrown units, see: (a) Yamauchi, A.; Hayashita, T.; Kato, A.; Teramae, N. *Bull. Soc. Chem. Jpn.* **2002**, *75*, 1527. (b) Kim, Y.-H.; Hong, J.-I. *Chem. Commun.* **2002**, 512. (c) Bekiari, V.; Judeinstein, P.; Lianos, P. *J. Luminescence* **2003**, *104*, 13.

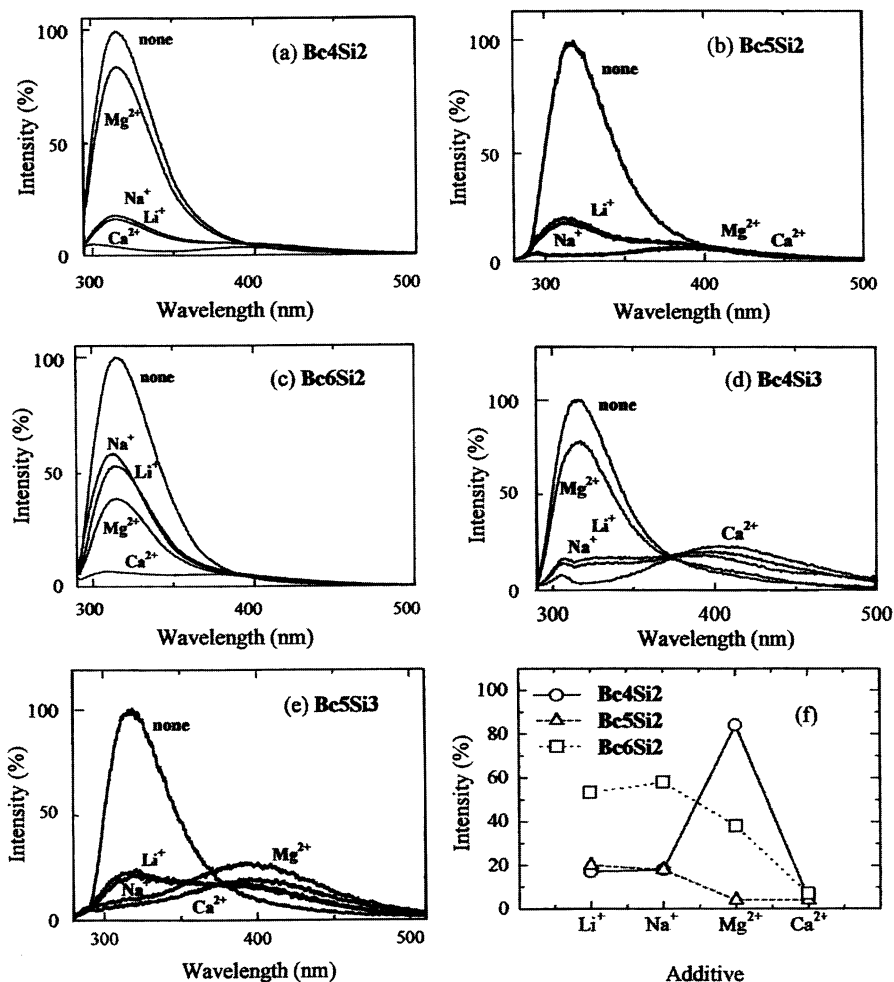


**Figure 1.** (a–e) Emission spectra of **BcnSi2** in the absence and presence of alkali and alkali-earth metal perchlorates ( $[\text{BcnSi2}] = 2.0 \times 10^{-5} \text{ M}$  in AN,  $[\text{metal perchlorate}]/[\text{BcnSi2}] = 1 \times 10^3$ ). (f) Relative emission intensities of **BcnSi2** at about 320 nm in the presence of metal ions, to those in the absence of the ions.

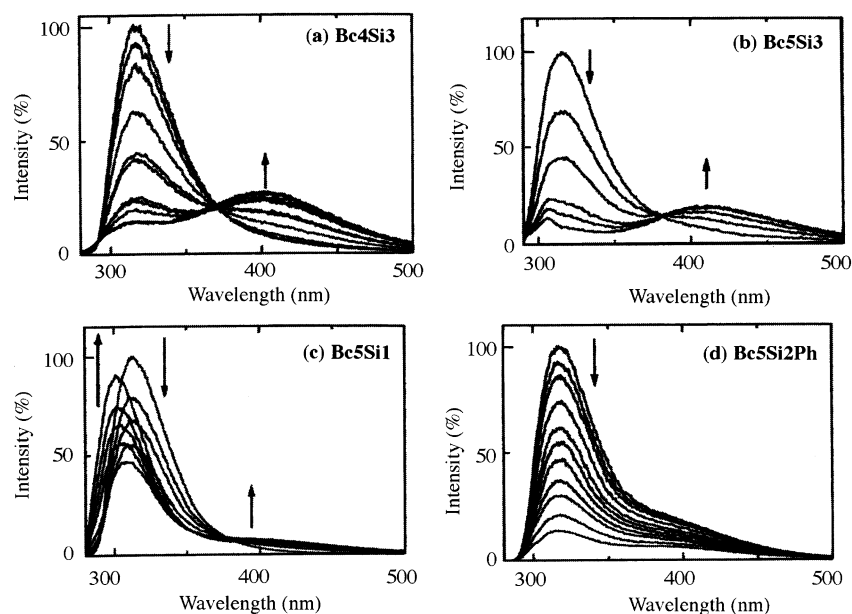


**Figure 2.** Emission spectral changes by titration of benzocrown derivatives (a) **Bc4Si3** with  $\text{Ca}(\text{ClO}_4)_2$  and (b) **Bc5Si3**, (c) **Bc5Si1**, and (d) **Bc5Si2Ph** with  $\text{Mg}(\text{ClO}_4)_2$  ( $[\text{substrate}] = 2.0 \times 10^{-5} \text{ M}$  in AN,  $[\text{M}(\text{ClO}_4)_2]/[\text{substrate}] = 0\text{--}2$ ).

$\text{Mg}^{2+}$  could be performed, respectively, in the presence of a  $1 \times 10^3$  fold excess of an interfering ion,  $\text{Mg}^{2+}$  or  $\text{Na}^+$  (Figure 3). Clear correlation between  $[\text{M}^{2+}]$  and

emission intensities was noted. The emission intensity of the low-energy broad band of **Bc5Si3** did not show evident changes depending on  $[\text{Mg}^{2+}]$  in the presence

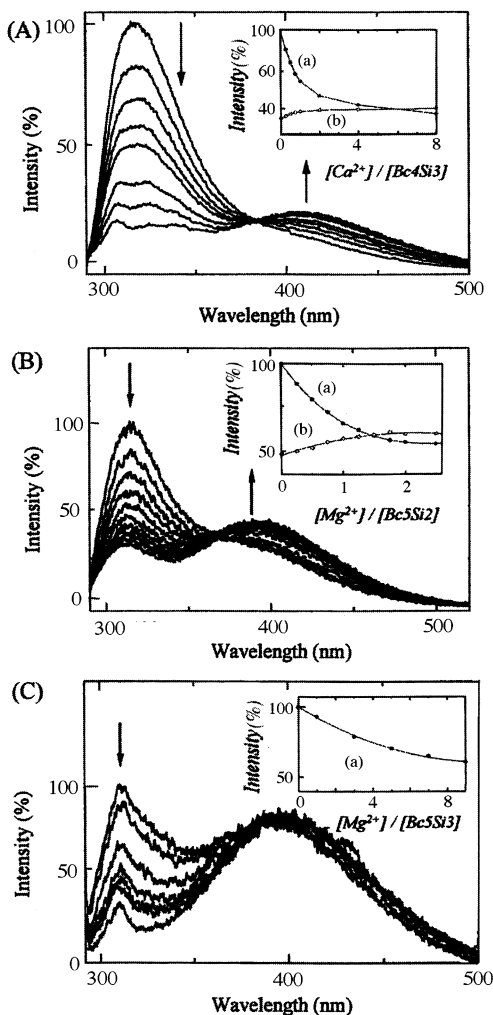


**Figure 3.** Emission spectral changes by titration of benzocrown derivatives (A) **Bc4Si3** with  $\text{Ca}(\text{ClO}_4)_2$  and (B) **Bc5Si2** and (C) **Bc5Si3** with  $\text{Mg}(\text{ClO}_4)_2$  in the presence of a large excess of (A)  $\text{Mg}(\text{ClO}_4)_2$  or (B, C)  $\text{Na}(\text{ClO}_4)$  ([metal perchlorate]/[**BcnSix**] =  $1 \times 10^3$ ). Insets show plots of emission intensities of the bands at (a) 315 nm and (b) 400 nm vs  $[\text{M}^{2+}]/[\text{BcnSix}]$  ( $\text{M} = \text{Mg}$  or  $\text{Ca}$ ).

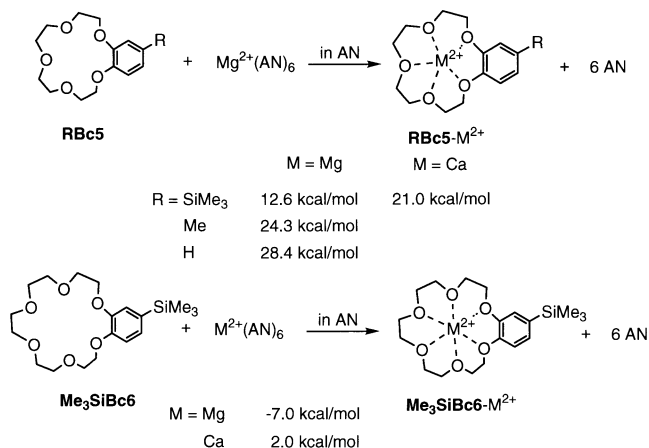
of an excess of  $\text{Na}^+$ , unlike **Bc5Si2**. In this case, only the higher energy emission underwent a continuous change of the intensity.

Monosilanylene-bridged and disilanyl-substituted benzocrown derivatives (**Bc5Si1** and **Bc5Si2Ph**) exhibited chromism toward  $\text{Mg}^{2+}$  ion, in different fashions from that observed for **BcnSix** ( $x = 2$  or  $3$ ). Thus, the emission intensity of **Bc5Si1** in AN first decreased with increasing  $[\text{Mg}^{2+}]$ , then increased, accompanied with a slight blue shift of the maximum from 312 to 300 nm (Figure 2c). No emission bands in the lower energy region appeared in these experiments. The emission spectrum of **Bc5Si2Ph** revealed a maximum at 317 nm with a shoulder at 390 nm in the absence of ions. Addition of  $\text{Mg}^{2+}$  to its AN solution led to a monotonic decrease of the emission intensity, as shown in Figure 2d. Neither the emission band nor shoulder was shifted.

## Discussion

The results described above clearly showed that the presence of two benzocrown ether units linked by a di- or trisilane linkage was necessary to realize both a

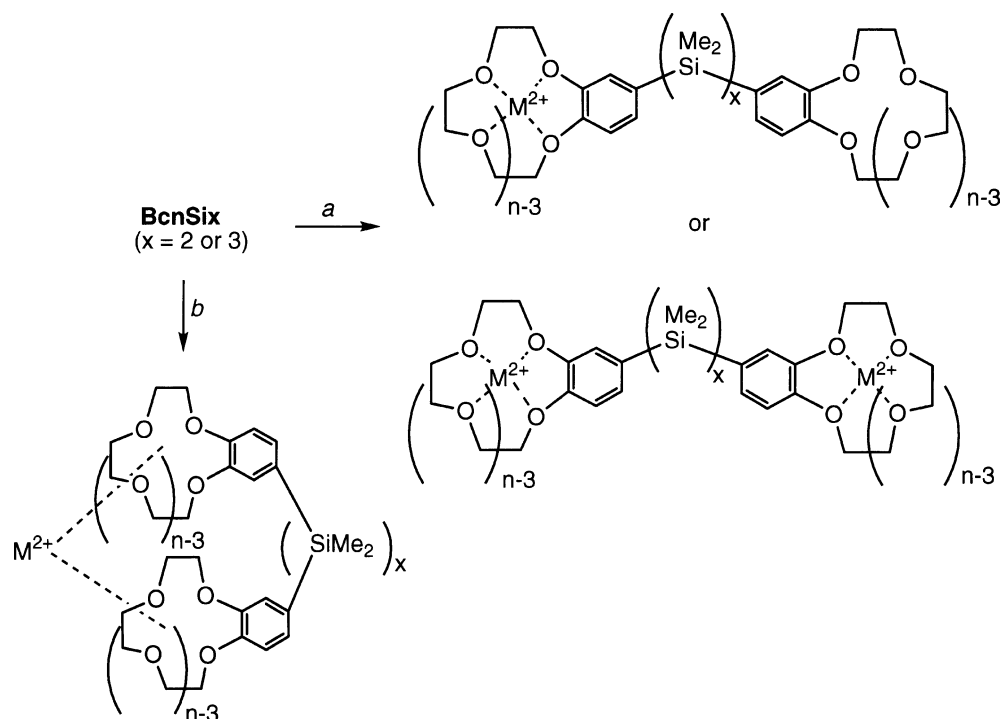
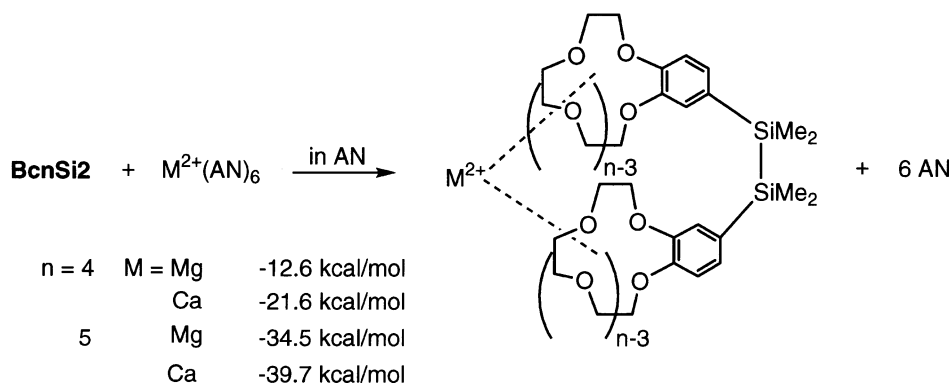
## Scheme 2. Model Reactions and Their Reaction Heats ( $\Delta H$ ) in AN, Derived from MO Calculations at the RHF/6-31+G Level, Using the Onsager Model



decrease of the original emission intensities and the appearance of a new band in the lower energy region on addition of metal ions. This is best explained in terms of the formation of excimers and/or exciplexes arising from  $\pi$ - $\pi$  stacking. The concentration of the substrates did not affect the profiles of the spectral changes, indicating that the changes originated from the intramolecular stacking of the chromophores, but not from any of the intermolecular processes. The fact that the absorption spectra were only a little affected by the presence of metal ions, in contrast to the emission spectra, indicated that the ionochromic effects worked well only in the excited states, agreeing with the excimer and/or exciplex formation. This also indicated that the no significant ionochromic effects on the  $\sigma$ - $\pi$  conjugation were involved in the present system.

To know more about the ionochromism, we carried out MO calculations on model reactions in AN, shown in Scheme 2. All calculations were performed at the HF/6-31+G level using the Onsager (dipole and sphere) model for inclusion of solvent in the calculations (see Experimental Section). Counteranions were omitted. Coordination numbers of  $\text{Mg}^{2+}$  and  $\text{Ca}^{2+}$  with AN were determined to be 6 each, by comparison of reaction heats of  $\text{M}^{2+} + n(\text{AN}) \rightarrow \text{M}^{2+}(\text{AN})_n$  in AN. As shown in Scheme 2, the formation of a 1:1 complex of benzocrown derivatives (**RBc5**) with  $\text{Mg}^{2+}$  was calculated to be endothermic and was preferred by substitution of the benzene ring with  $\text{R} = \text{Me}$  and  $\text{SiMe}_3$ , probably due to the electron-donating properties of these substituents, which would increase electron densities of the crown ether unit. Changing the metal from  $\text{Mg}$  to  $\text{Ca}$  resulted in less favored formation of the complex for **Me<sub>3</sub>SiBc5**, indicating an important role of the metal ion size.

In contrast to **Me<sub>3</sub>SiBc5**- $\text{Mg}^{2+}$ , the formation of **Me<sub>3</sub>SiBc6**- $\text{Mg}^{2+}$  was calculated to be a little exothermic. In this reaction, preferred size match between  $\text{Mg}^{2+}$  and the crown ether ring as well as the existence of enough coordination sites in **Me<sub>3</sub>SiBc6** seem to provide the energy gain. On the other hand, the formation of **Me<sub>3</sub>SiBc6**- $\text{Ca}^{2+}$  was computed to be again endothermic. Scheme 3 shows three possible coordination modes of the present system. In path *a*, no strong interaction between two benzocrown units can be expected, while in path *b*, the formation of  $\pi$ - $\pi$  stacking is likely to

**Scheme 3.** Three Possible Types of Coordination of **BcnSix** with  $M^{2+}$ **Scheme 4.** Reaction Heats ( $\Delta H$ ) for 1:1 Complex Formation in AN, Derived from MO Calculations at the RHF/6-31+G//RHF/6-31G Level, Using the Onsager Model

occur. Presumably, for **Bc6Si2** the formation of a chelate-type 1:1 complex with  $Mg^{2+}$  that originates the  $\pi$ - $\pi$  stacking is not as favored as that with  $Ca^{2+}$ , since  $Mg^{2+}$  can form a stable complex by coordination with one of the benzocrown units (path *a*). With  $Ca^{2+}$ , which is larger in size, however, it seems to be necessary to use both of the units in a chelate fashion to form a stable complex (path *b*). This seems to be responsible for the higher sensitivity of **Bc6Si2** in recognition of  $Ca^{2+}$  with respect to the emission spectra, relative to the case of  $Mg^{2+}$ .

Scheme 4 summarizes the results of MO calculations for 1:1 complex formation between **BcnSi2** ( $n = 4$  or  $5$ ) and  $M^{2+}$  ( $M = \text{Mg}$  or  $\text{Ca}$ ). In these calculations, the geometries were optimized at the HF/6-31G level and the energy calculations were performed at the HF/6-31+G level on the optimized geometries. On optimization of the structures of the starting **Bc4Si2**, two conformers were found to be stable with an energy minimum. One possesses two benzocrown groups in an anti fashion with respect to the disilanylene unit, while the other bears them in a gauche form. The former was

calculated to be more stable in a vacuum, but less stable in AN, as compared with the latter. Therefore, reaction heats shown in Scheme 3 are based on the gauche conformers for both **Bc4Si2** and **Bc5Si2**. In good agreement with the experimental results, these reactions were calculated to be exothermic and coordination of **Bc4Si2** with  $Ca^{2+}$  was found to be more favored than that with  $Mg^{2+}$ . This is probably due to the smaller ion size of  $Mg^{2+}$ . In fact, the Si-Si-C(sp<sup>2</sup>) angles in the optimized geometries of **Bc4Si2**- $Mg^{2+}$  are 104.39° and 104.29°, smaller than those in **Bc4Si2**- $Ca^{2+}$  (105.23° and 105.07°), indicating the larger strain energy in **Bc4Si2**- $Mg^{2+}$ .

Figure 4 depicts the optimized geometries of **Bc4Si2**- $Mg^{2+}$  and **Bc5Si2**- $Mg^{2+}$ , derived from the calculations. In contrast to **Bc4Si2**- $Ca^{2+}$  and **Bc4Si2**- $Mg^{2+}$ , in which all of the oxygen atoms coordinate to the metal center with O- $M^{2+}$  distances shorter than 2.4 Å for  $M = \text{Mg}$  and 2.6 Å for  $M = \text{Ca}$  (Figure 4a), only six of 10 oxygen atoms are located closely to  $Mg^{2+}$  in **Bc5Si2**- $Mg^{2+}$  (Figure 4b). This loose binding leads to less strain in **Bc5Si2**- $Mg^{2+}$  than in **Bc4Si2**- $Mg^{2+}$ , as indicated by

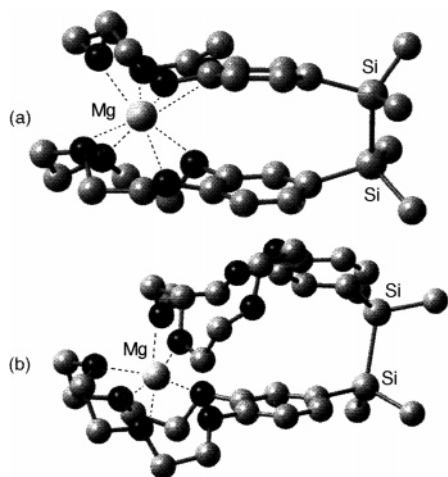


**Figure 4.** Optimized geometries of (a) **Bc4Si2**-Mg<sup>2+</sup> and (b) **Bc5Si2**-Mg<sup>2+</sup>, derived from MO calculations at the HF/6-31G level. The Onsager model with a dielectric constant of 36.64 (AN) was applied to include the solvent effects.

**Table 1. Apparent Binding Constants ( $K_s$ ) of BcnSix with Mg<sup>2+</sup> and Ca<sup>2+</sup> (M<sup>-1</sup>)<sup>a</sup>**

compd	Mg <sup>2+</sup>	Ca <sup>2+</sup>
<b>Bc4Si2</b>	nd <sup>b</sup>	$3.5 \times 10^4$
<b>Bc4Si3</b>	nd <sup>b</sup>	$1.1 \times 10^5$
<b>Bc5Si2</b>	$1.5 \times 10^5$	nd <sup>b</sup>
<b>Bc5Si3</b>	$2.3 \times 10^5$	nd <sup>b</sup>
<b>Bc6Si2</b>	nd <sup>b</sup>	$3.8 \times 10^6$

<sup>a</sup> Determined by emission spectra in acetonitrile. <sup>b</sup> Not determined.

larger Si–Si–C(sp<sup>2</sup>) angles in **Bc5Si2**-Mg<sup>2+</sup> (110.49° and 107.73°), making the chelate-type complex formation of **Bc5Si2** more favorable than that of **Bc4Si2**. As in the case of **Bc4Si2**, the formation of **Bc5Si2**-Ca<sup>2+</sup> was calculated to be preferred to that of **Bc5Si2**-Mg<sup>2+</sup>. However, the difference of the reaction heats seems to be too small to realize the selective response of **Bc5Si2** toward Mg<sup>2+</sup> and Ca<sup>2+</sup>.

The apparent binding constants ( $K_s$ ) of **BcnSix** with Mg<sup>2+</sup> and Ca<sup>2+</sup> were obtained by assuming that only the 1:1 chelate-type complex formation (path *b* in Scheme 3) had occurred during the emission spectral changes (see Experimental Section), as listed in Table 1. The binding constants for **BcnSi3** are higher than **BcnSi2** ( $n = 4$  and  $5$ ), indicating that flexible structure is important to hold the metal ion tightly. The highest constant is obtained for **Bc6Si2** with Ca<sup>2+</sup>. It should be noted that the  $K_s$  values for **Bc5Six** ( $x = 2$  and  $3$ ) with Mg<sup>2+</sup> are much higher than that of simple **Hbc5** with Mg<sup>2+</sup> in AN, reported previously ( $\log K = 4.48 \pm 0.03$ ).<sup>11</sup> Attempts to obtain the constants for **Bc5Six** ( $x = 2$  and  $3$ ) with Ca<sup>2+</sup> failed.

## Conclusions

We synthesized and characterized a series of organosilanyl-bridged benzocrown derivatives, which are able to respond to the selected metal ions with respect to the emission spectra. However, the UV spectra were not significantly affected by the coexistence of metal ions, in contrast to our expectation that interaction between the benzocrown units with the ions would

change the nature of the  $\sigma$ - $\pi$  conjugation in these molecules. It is noteworthy that the di- and trisilanyl-bridged ones emit visible blue luminescence in the presence of the metal ions. Although carbon-bridged benzocrown derivatives have been studied with respect to the ionochromic UV absorption behaviors as well as extraction of alkali ions from aqueous solutions,<sup>12</sup> the present silicon-bridged ones may be potentially useful as novel selective ion-sensors.

## Experimental Section

**General Procedures.** All reactions were carried out in dry nitrogen. THF was dried over sodium–potassium alloy and distilled just before use. Bromobenzocrown ethers were prepared as reported in the literature.<sup>13</sup>

**Preparation of Bc4Si2.** In a 50 mL Schlenk tube were placed 1.30 g (4.35 mmol) of (1-bromo-3,4-benzo)-12-crown-4 and 30 mL of THF, and the tube was cooled to  $-90$  °C. To this was added dropwise 3.13 mL (4.90 mmol) of a 1.57 M *n*-butyllithium-hexane solution, and the resulting mixture was stirred at this temperature for 10 min. After addition of 0.408 g (2.18 mmol) of 1,2-dichlorotetramethyldisilane, the mixture was allowed to warm to room temperature. The mixture was then hydrolyzed with water. The organic layer was separated, and the aqueous layer was extracted with ether. The organic layer and the extracts were combined and dried over anhydrous magnesium sulfate. After evaporation of the solvent, the residue was subjected to recycling preparative GPC (Shodex HF-801 and 802, 5 cm  $\phi \times 60$  cm each) eluting with benzene to give 0.578 g (47% yield) of **Bc4Si2** as colorless solids: mp 102–104 °C; MS *m/z* 562 (M<sup>+</sup>); <sup>1</sup>H NMR ( $\delta$  in CDCl<sub>3</sub>) 0.27 (s, 12H), 3.79 (s, 8H), 3.81–3.87 (m, 8H), 4.10 (t, 4H,  $J = 3.96$  Hz), 4.15 (t, 4H,  $J = 3.96$  Hz), 6.88–6.96 (m, 6H); <sup>13</sup>C NMR ( $\delta$  in CDCl<sub>3</sub>) –3.81, 69.88, 71.00, 71.27, 72.18 (2C), 117.02, 123.81, 128.68, 132.45, 149.90, 151.14; <sup>29</sup>Si NMR ( $\delta$  in CDCl<sub>3</sub>) –21.97. Anal. Calcd for C<sub>28</sub>H<sub>42</sub>O<sub>8</sub>Si<sub>2</sub>: C, 59.75; H, 7.52. Found: C, 59.73; H, 7.48.

Other silicon-substituted benzocrown derivatives were prepared as above using the corresponding chlorosilanes and lithiated benzocrown ethers.

**Data for Bc4Si3:** colorless solids; mp 77–80 °C; MS *m/z* 620 (M<sup>+</sup>); <sup>1</sup>H NMR ( $\delta$  in CDCl<sub>3</sub>) 0.04 (s, 6H), 0.22 (s, 12H), 3.79 (br s, 8H), 3.82–3.88 (m, 8H), 4.13–4.17 (m, 8H), 6.92–6.97 (m, 6H); <sup>13</sup>C NMR ( $\delta$  in CDCl<sub>3</sub>) –6.45, –3.09, 69.96, 70.01, 71.07, 71.41, 72.40 (2C), 117.04, 123.88, 128.73, 133.19, 149.97, 151.20; <sup>29</sup>Si NMR ( $\delta$  in CDCl<sub>3</sub>) –18.49, –48.26. Anal. Calcd for C<sub>30</sub>H<sub>48</sub>O<sub>8</sub>Si<sub>3</sub>: C, 58.02; H, 7.79. Found: C, 57.85; H, 7.94.

**Data for Bc5Si2:** colorless solids mp 91–92 °C; MS *m/z* 650 (M<sup>+</sup>); <sup>1</sup>H NMR ( $\delta$  in CDCl<sub>3</sub>) 0.27 (s, 12H), 3.74 (s, 16H), 3.86–3.90 (m, 8H), 4.02 (t, 4H,  $J = 4.23$  Hz), 4.10 (t, 4H,  $J = 4.23$  Hz), 6.80 (br s, 2H), 6.81 (d, 2H,  $J = 7.73$  Hz), 6.89 (dd, 2H,  $J = 7.73$ , 1.11 Hz); <sup>13</sup>C NMR ( $\delta$  in CDCl<sub>3</sub>) –3.75, 68.60, 69.11, 69.58, 69.65, 70.47, 70.56, 71.03 (2C), 113.36, 119.41, 127.42, 130.83, 148.50, 149.67; <sup>29</sup>Si NMR ( $\delta$  in CDCl<sub>3</sub>) –20.99. Anal. Calcd for C<sub>32</sub>H<sub>50</sub>O<sub>10</sub>Si<sub>2</sub>: C, 59.05; H, 7.74. Found: C, 58.99; H, 7.77.

**Data for Bc5Si1:** colorless solids mp 84–86 °C; MS *m/z* 592 (M<sup>+</sup>); <sup>1</sup>H NMR (CDCl<sub>3</sub>)  $\delta$  0.46 (s, 6H), 3.74 (s, 16H), 3.89 (s, 8H), 4.08–4.12 (m, 8H), 6.85 (d, 2H,  $J = 7.97$  Hz), 6.95 (s, 2H), 7.03 (d, 2H,  $J = 7.97$  Hz); <sup>13</sup>C NMR (CDCl<sub>3</sub>)  $\delta$  –1.97, 68.61, 69.26, 69.54, 69.66, 70.46, 70.58, 71.04 (2C), 113.29, 119.81, 127.98, 130.31, 148.55, 150.18; <sup>29</sup>Si NMR (CDCl<sub>3</sub>)  $\delta$

(12) (a) Lindsten, G.; Wennerström, O.; Thulin, B. *Acta Chem. Scand.* **1986**, *B40*, 545. (b) Kikukawa, K.; He, G.-X.; Abe, A.; Arata, R.; Ikeda, T.; Wada, F.; Matsuda, T. *J. Chem. Soc., Perkin Trans. 2* **1987**, 135.

(13) Okano, T.; Iwahara, M.; Konishi, H.; Kiji, J. *J. Organomet. Chem.* **1988**, *346*, 267.

(11) Shamsipur, M.; Madrakian, T. *J. Coord. Chem.* **2000**, *52*, 139.

–8.07. Anal. Calcd for C<sub>30</sub>H<sub>44</sub>O<sub>10</sub>Si: C, 60.79; H, 7.48. Found: C, 60.74; H, 7.48.

**Data for Bc5Si3:** colorless solids; mp 78–80 °C; MS *m/z* 708 (M<sup>+</sup>); <sup>1</sup>H NMR (δ in CDCl<sub>3</sub>) 0.03 (s, 6H), 0.23 (s, 12H), 3.75 (s, 16H), 3.90 (t, 8H, *J* = 4.23 Hz), 4.09–4.13 (m, 8H), 6.82 (d, 2H, *J* = 7.85 Hz), 6.86 (s, 2H), 6.89 (d, 2H, *J* = 7.85 Hz); <sup>13</sup>C NMR (δ in CDCl<sub>3</sub>) –0.41, –3.01, 68.65, 69.34, 69.61, 69.73, 70.48, 70.61, 71.04, 71.08, 113.78, 119.58, 127.44, 131.52, 148.58, 149.72; <sup>29</sup>Si NMR (δ in CDCl<sub>3</sub>) –0.41, –3.01. Anal. Calcd for C<sub>34</sub>H<sub>56</sub>O<sub>10</sub>Si<sub>3</sub>: C, 57.59; H, 7.96. Found: C, 57.40; H, 7.99.

**Data for Bc6Si2:** colorless solids; mp 41–45 °C; MS *m/z* 738 (M<sup>+</sup>); <sup>1</sup>H NMR (δ in CDCl<sub>3</sub>) 0.27 (s, 12H), 3.67 (s, 8H), 3.70–3.76 (m, 16H), 3.87–3.93 (m, 8H), 4.05 (t, 4H, *J* = 4.62 Hz), 4.13 (t, 4H, *J* = 4.62 Hz), 6.82 (d, 2H, *J* = 1.32), 6.82 (d, 2H, *J* = 7.92 Hz), 6.89 (dd, 2H, *J* = 7.92, 1.32 Hz); <sup>13</sup>C NMR (δ in CDCl<sub>3</sub>) –3.68, 68.75, 69.17, 69.64, 69.72, 70.78 (6C), 113.53, 119.64, 127.49, 130.91, 148.39, 149.58; <sup>29</sup>Si NMR (δ in CDCl<sub>3</sub>) –20.01. Anal. Calcd for C<sub>36</sub>H<sub>58</sub>O<sub>12</sub>Si<sub>2</sub>: C, 58.51; H, 7.91. Found: C, 58.44; H, 7.97.

**Data for Bc5Si2Ph:** colorless oil; MS *m/z* 460 (M<sup>+</sup>); <sup>1</sup>H NMR (δ in CDCl<sub>3</sub>) 0.29 (s, 6H), 0.31 (s, 6H), 3.76 (s, 8H), 3.85–3.91 (m, 4H), 3.97–4.00 (m, 2H), 4.10–4.13 (m, 2H), 6.76 (d, 1H, *J* = 1.45 Hz), 6.82 (d, 1H, *J* = 7.97 Hz), 6.91 (dd, 1H, *J* = 7.97, 1.45 Hz); <sup>13</sup>C NMR (δ in CDCl<sub>3</sub>) –3.99, –3.75, 68.64, 69.06, 69.59, 69.65, 70.47, 70.56, 71.07, 71.08, 113.41, 119.49, 127.32, 127.65, 128.32, 130.63, 133.85, 139.16, 148.48, 149.68; <sup>29</sup>Si NMR (δ in CDCl<sub>3</sub>) –21.83, –22.04. Anal. Calcd for C<sub>24</sub>H<sub>36</sub>O<sub>5</sub>Si<sub>2</sub>: C, 62.57; H, 7.88. Found: C, 62.54; H, 7.79.

**MO Calculations.** All calculations were performed by using the Gaussian 98 suite of programs revision A9<sup>14a,b</sup> and the Gauss-View interface version 2.1.<sup>14a</sup> First, the gas-phase geometries were obtained at the HF/6-31G level. In the next step, the Onsager field model was used to include the solvent effects.<sup>15</sup> Thus, geometry optimizations were carried out with the molecules placed in a spherical cavity within a dielectric medium at the same level of the theory. In these calculations in AN, molecular geometries and volumes derived from the gas-phase calculations were employed as the initial inputs, and a dielectric constant of 36.64 was used for AN. Further geometry optimizations and energy calculations were carried out at the HF/6-31+G level to incorporate the diffuse function, for the mono-benzocrown derivatives and their complexes, the

AN molecule, and AN-coordinated metal ions. For the bis-benzocrown derivatives and their complexes, single-point energies were calculated at HF/6-31+G for the molecular geometries obtained by HF/6-31G calculations.

#### Determination of Apparent Binding Constants (*K<sub>s</sub>*).

On the basis of the assumptions that only the formation of the 1:1 chelate-type complex had occurred during the emission spectral changes along path *b* in Scheme 3, the emission intensity became  $Y = Y_0 + (Y_{\text{lim}} - Y_0)\{1 + C_M/C_L + 1/(K_s C_L) - [(1 + C_M/C_L + 1/(K_s C_L))^2 - 4C_M/C_L]^{1/2}\}$ , where  $Y_0$  was the initial emission intensity without metal ions,  $Y_{\text{lim}}$  was the limiting value of the intensity, and  $C_M$  and  $C_L$  were concentrations of the metals and benzocrown derivatives, respectively.<sup>16</sup> Fitting the theoretical curves, with  $Y_{\text{lim}}$  and  $K_s$  as floating parameters, to the experimental plots of  $C_M/C_L$  versus  $Y$  afforded the binding constants  $K_s$  listed in Table 1. Good fitting could not be obtained for the cases of **Bc5Six** ( $x = 2$  and 3) with Ca<sup>2+</sup>.

**Acknowledgment.** This work was supported in part by NEDO (project No. 01A26005a). We thank Sankyo Kasei Co. Ltd. and Mitsubishi Chemical Corporation Fund for the financial support.

OM0400907

(14) (a) Program Packages from Gaussian, Inc.: Pittsburgh, PA. (b) Frisch, M. J.; Trucks, G. W.; Schlegel, H. B.; Scuseria, G. E.; Robb, M. A.; Cheeseman, J. R.; Zakrzewski, V. G.; Montgomery, J. A., Jr.; Stratmann, R. E.; Burant, J. C.; Dapprich, S.; Millam, J. M.; Daniels, A. D.; Kudin, K. N.; Strain, M. C.; Farkas, O.; Tomasi, J.; Barone, V.; Cossi, M.; Cammi, R.; Mennucci, B.; Pomelli, C.; Adamo, C.; Clifford, S.; Ochterski, J.; Petersson, G. A.; Ayala, P. Y.; Cui, Q.; Morokuma, K.; Maliek, D. K.; Rabuck, A. D.; Raghavachari, K.; Foresman, J. B.; Cioslowski, J.; Ortiz, J. V.; Stefanov, B. B.; Liu, G.; Liashenko, A.; Piskorz, P.; Komaromi, I.; Gomperts, R.; Martin, R. L.; Fox, D. J.; Keith, T.; Al-Lalam, M. A.; Peng, C. Y.; Nanayakkara, A.; Gonzalez, C.; Challacombe, M.; Gill, P. M. W.; Johnson, B. G.; Chen, W.; Wong, M. W.; Andres, J. L.; Head-Gordon, M.; Replogle, E. S.; Pople, J. A.

(15) (a) Onsager, L. *J. Am. Chem. Soc.* **1936**, *58*, 1486. For recent works using the Onsager model calculations, see: (b) Salter, E. A.; Wierzbicki, A.; Spearl, G.; Thompson, W. J. *Struct. Chem.* **2003**, *14*, 527. (c) Pasterny, K.; Wrzalik, R.; Kuoka, T.; Pasterna, G. *J. Mol. Struct.* **2002**, *614*, 297.

(16) Valeur, B. *Molecular Fluorescence*; Wiley-VCH: New York, 2002.